

A Design of Antenna Array with Improved Performance for Future Smartphones

Naser O. Parchin^{1, *}, Haleh J. Basherlou²,
Yasir I. A. Al-Yasir¹, and Raed A. Abd-Alhameed¹

Abstract—In this study, a new multiple-input-multiple-output (MIMO) antenna array is introduced for fifth-generation (5G) smartphones. Its schematic contains eight planar inverted F antenna (PIFA) elements placed at edges of the mobile-phone mainboard with a $75 \times 150 \times 0.8 \text{ mm}^3$ FR-4 substrate. The ground plane and antenna resonators are etched on the back layer of the mainboard. By employing arrow strips between the adjacent elements, the frequency bandwidth and isolation level of the PIFA radiators are improved. The proposed smartphone antenna array is designed to support the spectrum of commercial sub 6 GHz 5G communication and cover the frequency range of 3.25–3.85 GHz with isolation levels better than -15 dB . Due to the compact size and corner placements of the PIFAs, the presented MIMO antenna array occupies a small part of the board. In addition, the proposed smartphone antenna array provides not only sufficing radiation coverage supporting different sides of the mainboard but also the polarization diversity. The MIMO performance and characteristics of the proposed smartphone antenna design in the presence of the user phantom are also discussed.

1. INTRODUCTION

MIMO technology is a key feature and promising technology to obtain a higher transmission rate of future wireless communications [1, 2]. MIMO antenna is a significant facility to improve the channel capacity of the MIMO system [3, 4]. MIMO technology requires that all antenna radiators work simultaneously. Standard MIMO systems tend to employ two or four elements in a single physical package. However, a high number of antenna radiators are employed for the massive MIMO system [5, 6]. Compared with previous generations, a large number of antenna elements operating concurrently is expected to be applied for 5G communications [7]. 2×2 MIMO systems are successfully deployed for fourth-generation (4G) mobile communications, and it is expected that the massive MIMO system of 5G communications should be with a large number of MIMO antennas since greater number makes the system more resistant to interferences [8, 9]. The 5G network also needs fundamental technologies to enable small cells, beamforming, full duplexing, MIMO, and millimeter-wave (MM-Wave) [10–12].

Simple structure and compact antenna elements with sufficient impedance bandwidth and isolation are desirable to be integrated into 5G smartphone platforms [13, 14]. Several MIMO 5G smartphone antennas have been proposed recently [15–28]. However, these antennas either provide narrow bandwidth or occupy a huge space of mainboard. In [15–18], uniplanar and double-layer antenna elements with only 200 MHz bandwidths are proposed for 5G smartphone applications. A polarization-orthogonal co-frequency dual antenna pair with design complexity is proposed in [19] for metal-rimmed smartphones. In [20], a CPW-fed antenna array with large-clearance occupying huge space of smartphone board is introduced for sub 6 GHz MIMO handset. In [21] narrow-band antenna arrays

Received 20 January 2020, Accepted 2 April 2020, Scheduled 9 April 2020

* Corresponding author: Naser Ojaroudi Parchin (N.OjaroudiParchin@bradford.ac.uk).

¹ Faculty of Engineering and Informatics, University of Bradford, Bradford, United Kingdom. ² Bradford College, Bradford, United Kingdom.

with 100 MHz are represented to be integrated at the corners of the mainboard. The proposed antenna in [22] provides wide bandwidth. However, due to placements of the slot resonators in the ground plane, the proposed smartphone antenna does not provide enough space for display integration. A multi-element multi-layer antenna with the operation band of 4.4–4.7 GHz is proposed in [23]. The proposed antennas in [24–26] have uniplanar configurations which make them difficult to fabricate and integrate with the circuit system. In addition, the proposed 5G smartphone antenna array in [27] employs only six radiators which is not sufficient for 5G massive MIMO communication. Moreover, a high-isolated MIMO array with slot decoupling structures and 300 MHz bandwidth is reported in [28]. Its radiators are not planar, and careful consideration is required in the fabrication process. Among the 5G MIMO designs in the literature, our recently reported designs in [17] and [23] can also provide the polarization diversity function at different corners of the PCB. However, compared with them, the proposed MIMO antenna in this paper provides wider impedance bandwidth using compact antenna radiators. Also, unlike those double-layer designs with slot resonators, the proposed design is arranged in one-layer with ease of integration and possibility of more space for the smartphone display.

In order to have an efficient MIMO antenna system for user’s devices, some challenges have to be addressed. One of them is to design MIMO antenna elements with low-level isolation (mutual coupling) between the radiators placed in a confined space [29, 30]. Since decoupling is concerned, some techniques have been used to increase the isolation of MIMO elements while maintaining a compact design [31, 32], and one of the methods is to locate elements far apart. However, this technique may not be suitable for most smartphones. We present a new design method to enhance the isolation between these closely spaced elements and also to improve the bandwidth of the MIMO system for handsets. The antenna elements of the MIMO design are PIFAs fed by discrete ports extended from the ground plane to the radiator. The PIFA is a compact-size, light weight, and easy to fabricate antenna resonator with omnidirectional/quasi-omnidirectional radiation patterns that can be applied to different wireless systems [33, 34]. The proposed MIMO system is targeting at 3.5 GHz 5G candidate band and uses eight elements placed at different sides of the board [35]. The simulation is carried out using computer simulation technology (CST) software [36]. By adding arrow strips among the elements, the bandwidth and isolation of the MIMO system are improved. It provides more than 600 GHz bandwidth and less than -15 dB mutual couplings. This paper is structured as follows. The design and performance of the proposed MIMO antenna systems are represented in Section 2. Section 3 provides and compares the measurements with simulation. Section 4 investigates the behavior of the designed array in the vicinity of the user. Section 5 gives a conclusion of this manuscript.

2. ANTENNA DESIGN AND CHARACTERISTICS

The geometry of the designed MIMO diversity antenna design is given in Fig. 1. The smartphone antenna array is printed on a single-sided FR4 substrate with a thickness of 0.8 mm and relative permittivity of 4.4. The proposed MIMO antenna array is designed on a standard 5G mobile-phone PCB with an overall dimension of 75×150 mm². However, due to the small-clearance, low mutual coupling,

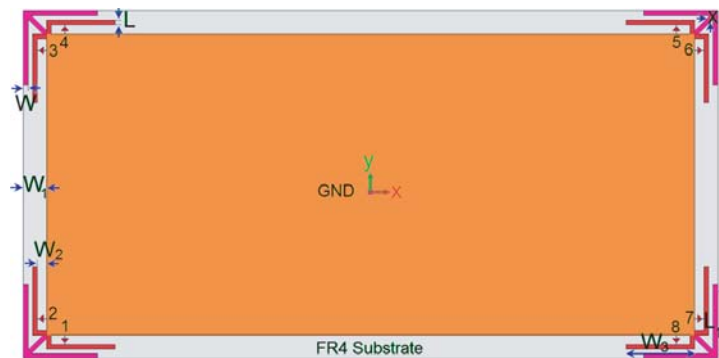


Figure 1. Configuration of the smartphone antenna array.

and compact sizes of the antenna elements, it is possible to integrate them on different commercially available cases, without any effect on the performance of the elements.

Large size of the ground plane could improve the isolation between elements and free more space for other circuit components. The design procedure for the presented MIMO antenna is simple and straight forward. First, conventional PIFA elements with low profiles are employed at different edges to provide diversity function. Then, in order to improve the impedance bandwidth and isolation of the radiators, arrow strips are inserted between adjacent elements, as illustrated in Fig. 1. Table 1 lists the dimensions of the proposed MIMO smartphone antenna.

Table 1. The values of the design parameters.

Parameter	W	L	W_1	L_1	W_2	W_3	x
Value (mm)	1	1	5	16	2	14.75	1

Figure 2 illustrates and compares the return loss (S_{11}) and mutual coupling (S_{21}) characteristics of two adjacent PIFAs without and with the arrow strip. It is shown that the arrow strip, placed between the elements, can act as a decoupling structure to increase the isolation between the antenna ports. Therefore, the mutual coupling has been successfully reduced from -8 to less than -15 dB. The employed strips improve not only the mutual coupling of the MIMO system but also the frequency bandwidth of the design [37–40]. As shown, compared with the conventional PIFA design (without the strips) the operation band of the proposed MIMO antenna has been increased significantly. The proposed design covers 600 MHz impedance bandwidth in the frequency spectrum of 3.25–3.85 GHz.

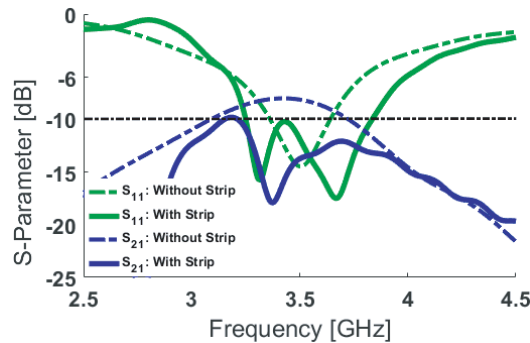


Figure 2. S_{11}/S_{21} of adjacent elements with/without the arrow-strip.

The frequency behavior and isolation of the designed array are flexible. The impedance matching and frequency tuning of the antenna for different values of the design parameters are discussed in Fig. 3. Fig. 3(a) illustrates S_{11} and S_{21} characteristics versus different values of W_3 varying from 14.74 to 10.75 mm. As seen, when its value changes, the lower and upper operation frequencies of the antenna increase from 3 to 3.5 GHz and 3.8 to 4.5 GHz, respectively. In addition, as can be observed, S_{21} function of the diversity antenna is tuned by changing the value of W_3 . However, as shown clearly, when $W = 12.75$ mm, the antenna exhibits a better and sufficient frequency response. Fig. 3(b) investigates the impedance matching function of the antenna for various values of L_1 : when its size changes from 18 to 14 mm, the matching characteristic of the diversity antenna varies from -9 dB to less than -30 dB. However, unlike S_{11} , S_{21} characteristic is almost constant with an insignificant variation.

Figure 4 illustrates S_{nn} (reflection coefficient) and S_{mn} (mutual-coupling) characteristics of the smartphone antenna array. As shown in Fig. 4(a), good S parameter results with a broad bandwidth of 600 MHz (3.3–3.9 GHz) for $S_{nn} \leq -10$ and 800 MHz (3.25–4 GHz) for $S_{nn} \leq 6$ dB are achieved for the design. Moreover, it provides sufficient mutual couplings between the elements, as depicted in Fig. 4(b). 3D transparent views of the radiation patterns at 3.5 GHz for each feeding port have been

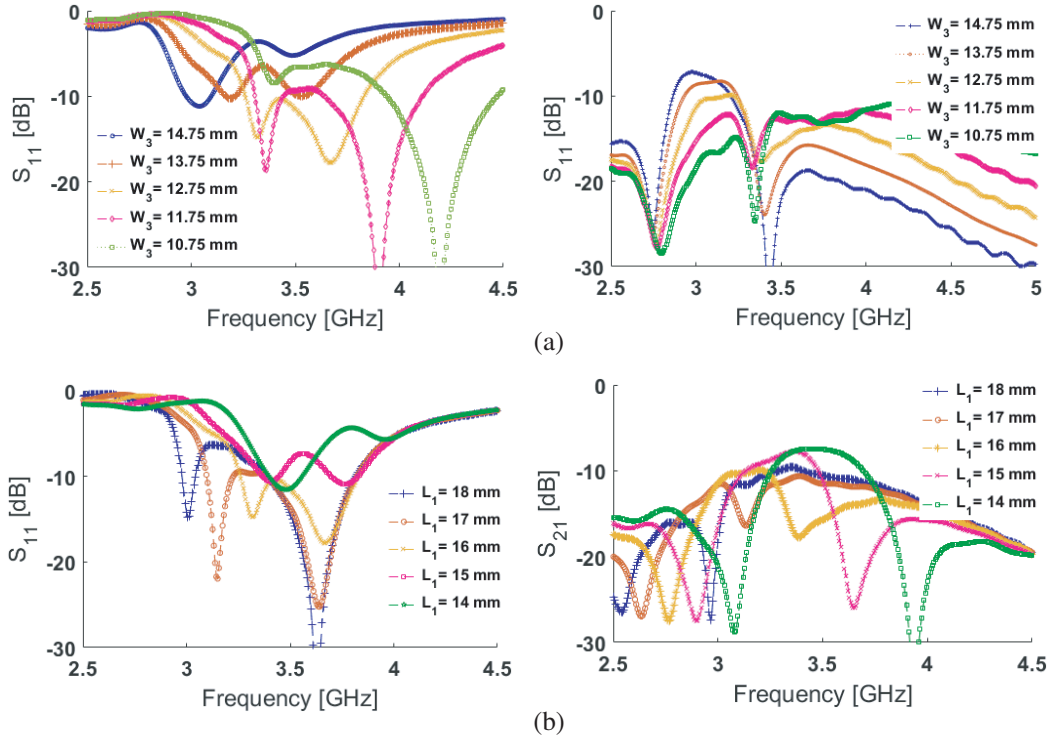


Figure 3. S_{11}/S_{21} results for different values of (a) W_2 and (b) L_2 .

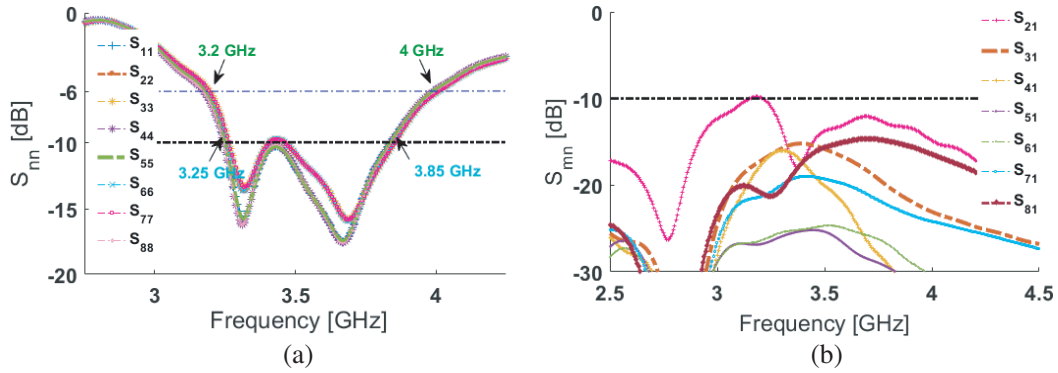


Figure 4. Simulated (a) S_{nn} and (b) S_{mn} of the array S -parameters.

illustrated in Fig. 5. It can be observed that the PIFA resonators could not only cover different sides of the mobile-phone board but also support different polarizations which is a unique function for MIMO design [41, 42]. It can be seen that the 8-element MIMO antenna can offer a sufficient gain value for each radiator. Moreover, four horizontally and vertically polarized radiation patterns are achieved to improve the MIMO performance of the design. The gain characteristic of the modified PIFAs is about 2.8–4 dB.

The efficiencies (radiation and total) of the PIFA resonators are also given in Figs. 6(a) and (b). It is shown that high efficiencies with slight variations are achieved within the range of 3.25–3.85 GHz. Besides, as seen, for the frequency range of 3.4–3.8 GHz, more than 80% radiation and 65% total efficiencies were observed for the proposed MIMO smartphone antenna design.

The total active reflection coefficient (TARC) and envelope correlation coefficient (ECC) specifications are two important parameters in diversity/MIMO antennas to justify that the antenna elements are competent for diversity reception/transmission in the MIMO channels [43, 44]. Fig. 7

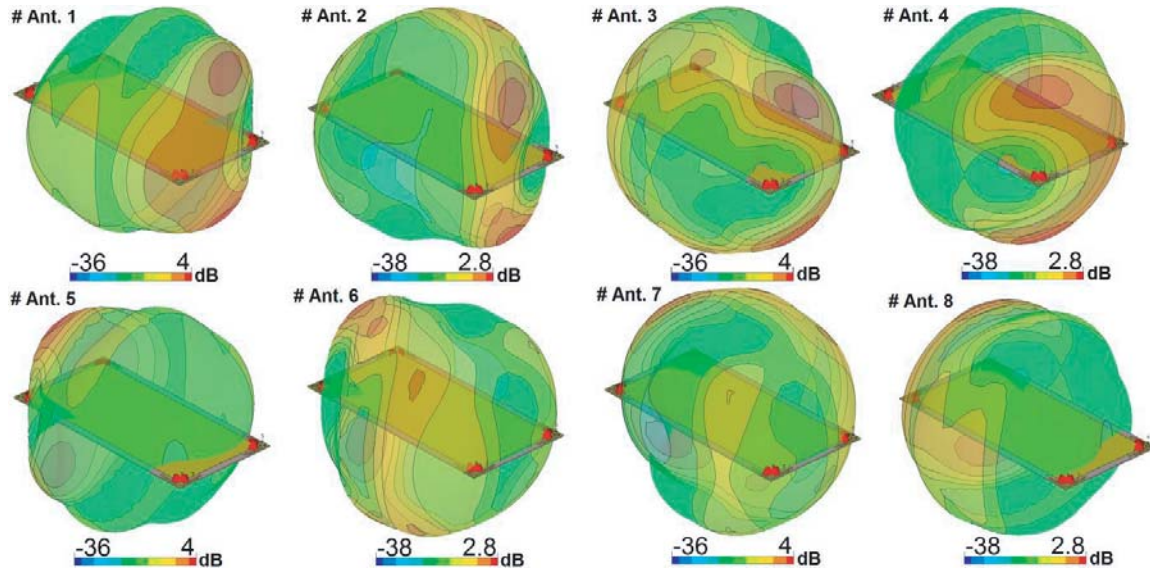


Figure 5. 3D radiation patterns of the PIFAs at 3.5 GHz.

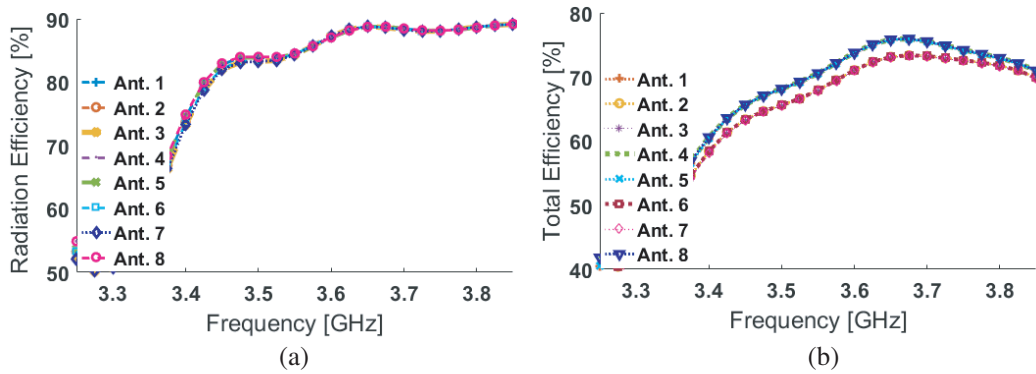


Figure 6. (a) Radiation and (b) total efficiencies of the MIMO design.

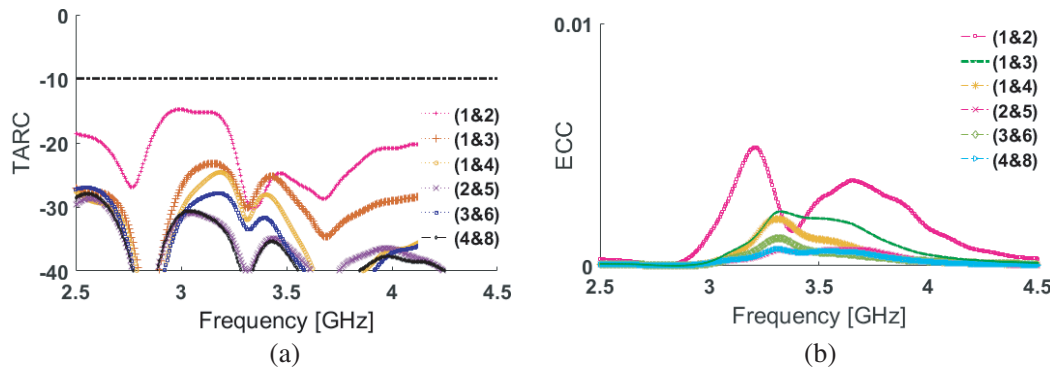


Figure 7. Calculated (a) TARC, (b) ECC results.

represents the calculated TARC and ECC results of the MIMO PIFA array. It is seen in Fig. 7(a) that the TARC results are less than -25 dB at 3.25–3.85 GHz (antenna operation band). Furthermore, as shown in Fig. 7(b), the calculated ECC characteristics of the array are very low over the band of interest with a maximum value of less than 0.005.

Table 2. Comparison between our design and the referenced 5G smartphone antennas.

Reference	Antenna Type	Bandwidth (GHz)	Efficiency (%)	Overall Size (mm ²)	Isolation (dB)	ECC
[15]	Coupled IFA	3.4–3.6	-	150 × 75	15	< 0.02
[16]	Inverted-F	3.4–3.6	55–60	100 × 50	10	-
[17]	Patch-Slot	3.55–3.65	52–76	150 × 75	11	-
[18]	Monopole	3.4–3.6	35–50	150 × 75	11	< 0.40
[19]	Spatial-Reuse Antenna	3.4–3.6	40–70	150 × 75	12	< 0.2
[20]	Inverted-L Monopole	3.4–3.6	40–60	136 × 68	14	< 0.2
[21]	Inverted-F	3.4–3.6	-	120 × 70	20	-
[22]	Ring-Slot	3.4–3.8	60–75	150 × 75	15	< 0.01
[23]	Monopole	4.55–4.75	50–70	136 × 68	10	-
[24]	Tightly Arranged Pairs	3.4–3.6	50–70	150 × 73	17	< 0.07
[25]	Wave-Guide	3.4–3.6	50–80	150 × 75	15	< 0.2
[26]	Monopole	3.4–3.6	60–70	150 × 75	18	< 0.015
[27]	open-end slot	3.4–3.6	50–60	136 × 68	11	0.05
[28]	loop element	3.3–3.6	40	120 × 70	15	0.02
This Work	Diversity PIFAs	3.25–3.85	40–75	150 × 75	15	< 0.01

Table 2 provides a comparison between the presented smartphone array antenna and some other reported smartphone arrays [15–28]. As can be observed, compared with the recently proposed 5G MIMO smartphone antennas with planar and uniplanar structures, our antenna has better performances in terms of impedance match and bandwidth, and its clearance size keeps at a satisfactory level, as shown in Table 2. The proposed design achieves not only around 0.6 GHz impedance bandwidth but also sufficient mutual couplings, better than -15 dB. Besides, unlike the reported 5G antenna design, our antenna is implemented in one-side of the smartphone mainboard which makes it easy to fabricate and integrate with the circuit.

3. FABRICATION AND MEASUREMENTS

A prototype sample of the proposed 5G smartphone antenna array was fabricated, as shown in Figs. 8(a) and (b). Due to similar placements and performances of the PIFA pairs, the properties of the smartphone antenna design for ports 1 and 2 are measured and compared in the following. The feeding mechanism of the adjacent PIFA elements is shown in Fig. 8(c). The measured and simulated results of the S -parameters are compared in Fig. 9. As seen, the measurements are in good agreement with the simulations to cover the required operation band: a quite good frequency bandwidth ($S_{11} < -10$ dB within 3.25–3.85 GHz), and mutual coupling ($S_{21} < -15$ dB) are obtained for the elements.

Measured and simulated 2D-polar radiation patterns of the closely-spaced PIFAs at 3.5 GHz (middle frequency) are shown in Fig. 10. It should be noted during the measurements, we keep one port excited and another loaded with a $50\text{-}\Omega$ load. As seen from Figs. 10(a) and (b), the prototype offers good quasi-omnidirectional radiation patterns with acceptable agreement between simulations and measurements [45, 46]. Fig. 11 shows the TARC and ECC results of the antenna pairs. As shown the obtained TARC result is less than -25 dB, and the ECC function is very low over the band of interest.

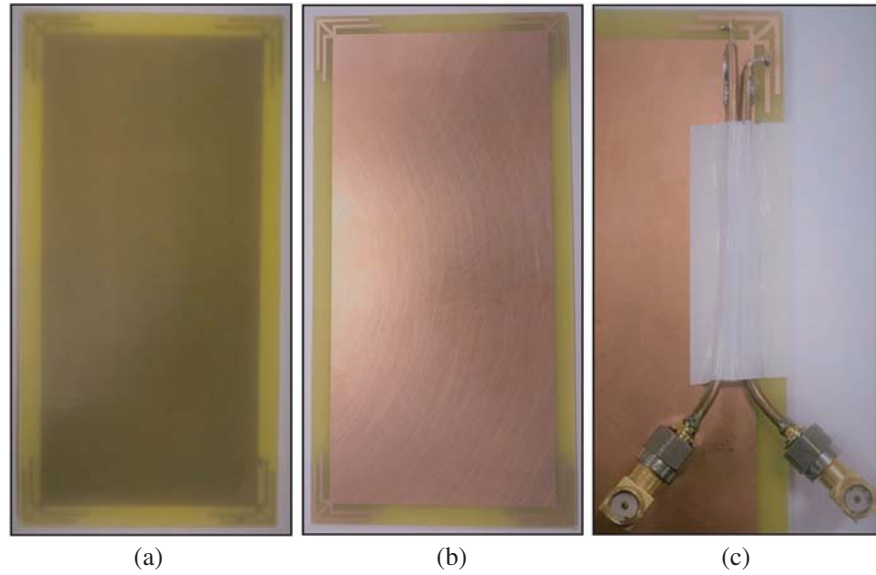


Figure 8. (a) Front (b) back views of the prototype sample, and (c) the feeding mechanism for two PIFAs.

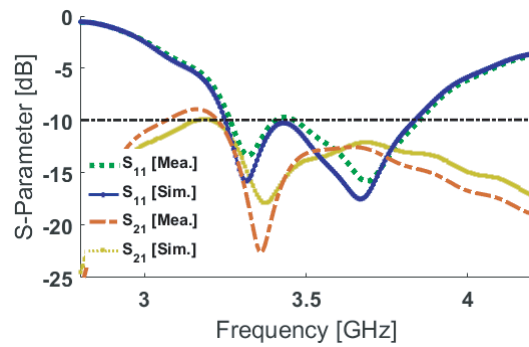


Figure 9. *S*-parameters of the adjacent PIFAs.

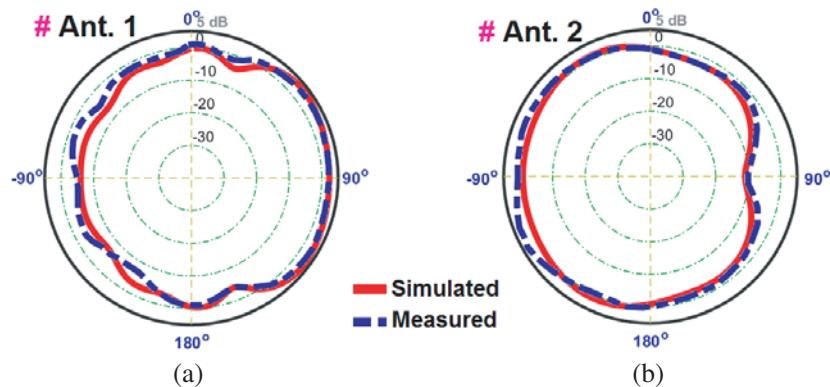


Figure 10. 2D polar radiation patterns at 3.5 GHz for Ports (a) 1 and (b) 2.

4. USER-EFFECT INVESTIGATION

The health hazard of emitted electromagnetic (EM) radiation from smartphones has become a point of open deliberation as the use of mobile handset increases exponentially [47, 48]. In this section, the

radiation performance of the presented 5G MIMO antenna in the vicinity of user-hand and user-head is studied. Standard Anthropomorphic Model (SAM) head is a homogeneous model of the human head composed of two parts: fluid and shell. It was created for measurements filled with head tissue-equivalent materials. The SAM phantom head and hand are provided by CST Microwave Studio software. The conductivity and relative dielectric constant properties of SAM head and hand models can be found in [49].

In the following, different usage postures in data-mode of the user-hand for right and left hands touching top/bottom sides of the smartphone are considered and studied in Fig. 12. The user-hand phantom in the data-mode has the relative permittivity of $\epsilon = 24$ and conductivity of $\sigma = 2\text{ s/m}$. According to the obtained results, the proposed design exhibits similar radiation behavior for different hand scenarios. This is mainly due to the symmetrical schematic of the designed MIMO antenna. It is shown that the smartphone antenna and its PIFA elements exhibit efficiencies of 25%–65%. It should be noted that due to the nature of hand tissue properties which can highly absorb the radiation power, some reduction in the antenna efficiency characteristics was expected. Compared with the reported 5G smartphone antennas in the literature, the proposed design provides good radiation and total efficiencies in the presence of user-hand. The maximum reductions of the total efficiencies are observed for the PIFA elements that have been partially covered by the hand [50, 51].

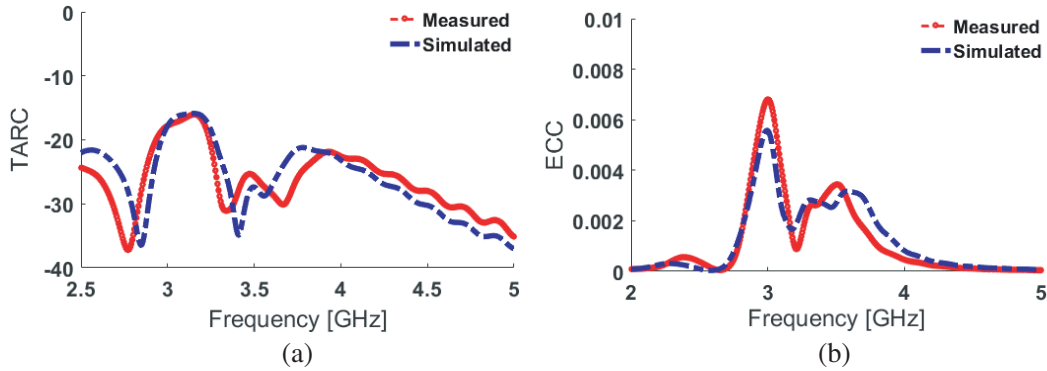


Figure 11. Calculated (a) TARC, (b) ECC results of the adjacent elements.

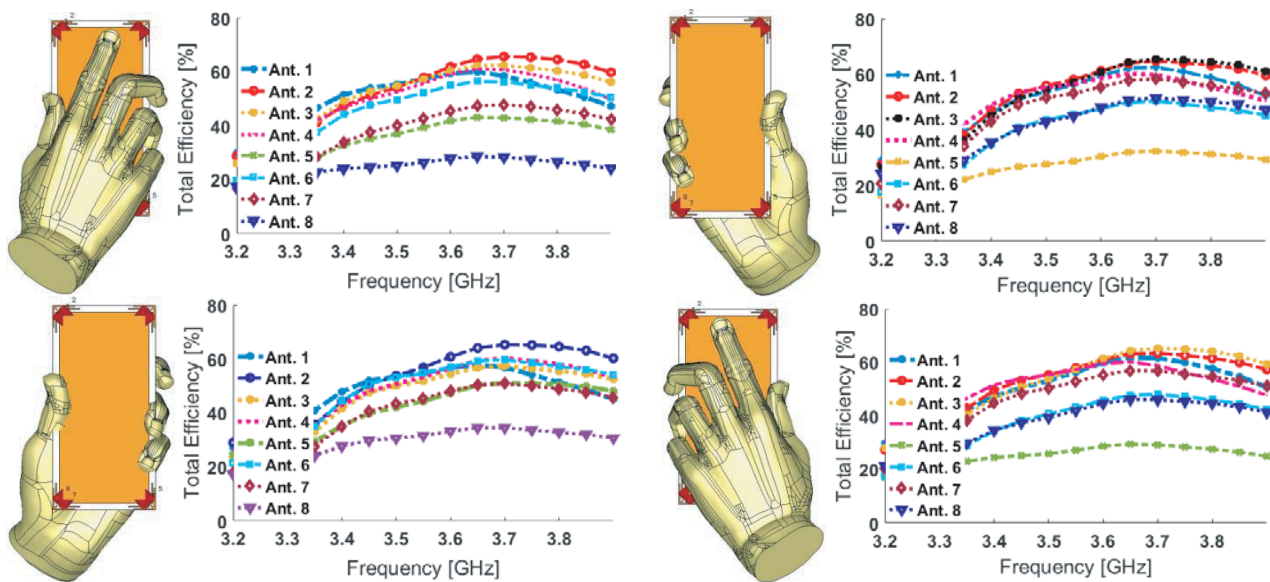


Figure 12. Placement and efficiencies of the PIFA array at different user-hand scenarios.

The EM energy absorbed by human body tissues can be evaluated by the specific absorption rate (SAR) [52, 53]. It is a measure of how much power is absorbed per unit mass. In smartphone antenna systems, for phased array designs such as millimeter-wave 5G antennas, the SAR of the main radiation beams (when multiple identical antenna elements with linear or planar form are excited) should be considered. Unlike the phased array design, each radiation element of the MIMO antenna system can work separately as a transmitter and receiver. Therefore, the SAR function of each element should be studied. The SAR features of the PIFA elements of the proposed MIMO design are investigated, and only the SAR functions of the antenna elements with maximum and minimum values are represented in Fig. 13(a): It is shown that Ant. 3 causes the maximum SAR value, and the minimum SAR value is observed from Ant. 7. According to the obtained results, the distance between the PIFA elements and the head phantom plays a main role in the value of the SAR function. In addition, as seen in Fig. 13 (b), the proposed design exhibit good S_{nn} ($S_{11} \sim S_{88}$) results in Talk-mode.

The radiation pattern results for the MIMO smartphone antenna in Talk-mode are shown in Fig. 14. As can be realized from the simulation, the proposed MIMO antenna offers good radiation patterns in Talk-mode. In addition, the gain levels of the antenna resonators vary from 1.5 to 3 GHz. This variation is mainly due to the presence of the user’s hand and head. As mentioned earlier, the user’s hand and head usually have negative effects on the characteristics of smartphone antennas and can reduce gain and efficiency levels of the antenna elements. Compared with Fig. 8, the maximum reduction of antenna gain is observed for the elements closely spaced with the user’s head and hand. In general, for the closer distance between the antenna element and the user-hand/head, the greater reduction on the gain and efficiencies will be expected [53–55].

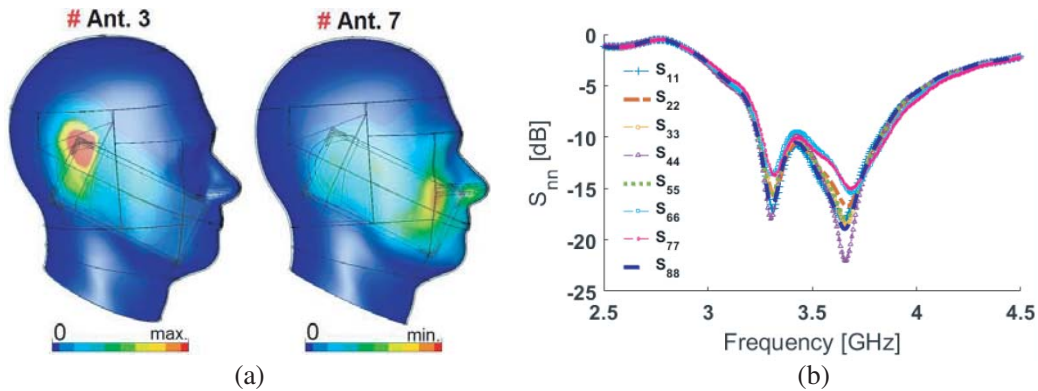


Figure 13. (a) SAR and (b) reflection coefficients in Talk-Mode.

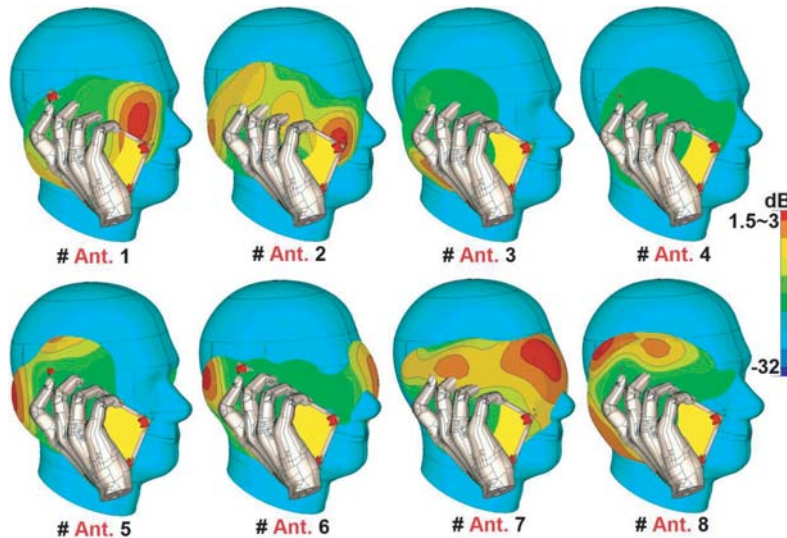


Figure 14. Radiation patterns at 3.5 GHz in Talk-Mode.

5. CONCLUSION

A 5G smartphone antenna array with improved characteristics is introduced in this paper. Four pairs of the discrete-fed PIFA antennas are placed at four corners of the mainboard to form an 8×8 MIMO antenna. By adding arrow strips between adjacent elements, the frequency bandwidth and isolation level of the MIMO system are improved significantly. Fundamental characteristics and MIMO performance of the design are investigated. It offers good characteristics in terms of bandwidth, isolation, and radiation pattern. A prototype sample of the design was fabricated, and characteristics of two adjacent PIFA elements were measured. Furthermore, the characteristics of the design in the presence of the user are discussed.

ACKNOWLEDGMENT

This work is supported by the European Union's Horizon 2020 research and innovation program under grant agreement H2020-MSCA-ITN-2016 SECRET-722424.

REFERENCES

1. Nadeem, Q. U. A., et al., "Design of 5G full dimension massive MIMO systems," *IEEE Trans. Commun.*, Vol. 66, 726–740, 2018.
2. Yang, H. H. and Y. Q. S. Quel, "Massive MIMO meet small cell," *SpringerBriefs in Electrical and Computer Engineering*, 2017, DOI 10.1007/978-3-319-43715-6_2.
3. Osseiran, A., et al., "Scenarios for 5G mobile and wireless communications: The vision of the METIS project," *IEEE Commun. Mag.*, Vol. 52, 26–35, 2014.
4. Parchin, N. O., et al., *Microwave/RF Components for 5G Front-end Systems*, 1–200, Avid Science, 2019.
5. Parchin, N. O. and R. A. Abd-Alhameed, "A compact Vivaldi antenna array for 5G channel sounding applications," *EuCAP*, 846, London, UK, 2018.
6. Ojaroudi, N., H. Ojaroudi, and N. Ghadimi, "Quad-band planar inverted-F antenna (PIFA) for wireless communication systems," *Progress In Electromagnetics Research Letters*, Vol. 45, 51–56, 2014.
7. Oliveri, G., et al., "Codesign of unconventional array architectures and antenna elements for 5G base stations," *IEEE Trans. Antennas Propag.*, Vol. 65, No. 12, 6752–6767, Dec. 2017.
8. Habaebi, M. H., M. Janat, and M. R. Islam, "Beam steering antenna array for 5G telecommunication systems applications," *Progress In Electromagnetics Research M*, Vol. 67, 197–207, 2018.
9. Comisso, M., et al., "3D multi-beam and null synthesis by phase-only control for 5G antenna arrays," *Electronics*, Vol. 8, 656, 2019.
10. Parchin, N. O., R. A. Abd-Alhameed, and M. Shen, "A radiation-beam switchable antenna array for 5G smartphones," *2019 Photonics & Electromagnetics Research Symposium — Fall (PIERS — Fall)*, 1769–1774, Xiamen, China, Dec. 17–20, 2019.
11. Parchin, N. O., R. A. Abd-Alhameed, and M. Shen, "A substrate-insensitive antenna array with broad bandwidth and high efficiency for 5G mobile terminals," *2019 Photonics & Electromagnetics Research Symposium — Fall (PIERS — Fall)*, 1764–1768, Xiamen, China, Dec. 17–20, 2019.
12. Jaber, M., M. A. Imran, R. Tafazolli, and A. Tukmanov, "5G backhaul challenges and emerging research directions: A survey," *IEEE Access*, Vol. 4, 1743–1766, Apr. 2016.
13. Chen, Q., et al., "Single ring slot based antennas for metal-rimmed 4G/5G smartphones," *IEEE Trans. Antennas Propag.*, Vol. 67, 1476–1487, 2018.
14. Ojaroudiparchin, N., et al., "Wide-scan phased array antenna fed by coax-to-microstriplines for 5G cell phones," *21st International Conference on Microwaves, Radar and Wireless Communications*, Krakow, Poland, 2016.

15. Liu, Y., et al., "MIMO antenna array for 5G smartphone applications," *13th European Conference on Antennas and Propagation (EuCAP 2019)*, Krakow, Poland, 2019.
16. Al-Hadi, A. A., J. Ilvonen, R. Valkonen, and V. Viikan, "Eight-element antenna array for diversity and MIMO mobile terminal in LTE 3500 MHz band," *Microwave Opt. Technol. Lett.*, Vol. 56, 1323–1327, 2014.
17. Ojaroudi Parchin, N., et al., "Dual-polarized MIMO antenna array design using miniaturized self-complementary structures for 5G smartphone applications," *13th European Conference on Antennas and Propagation (EuCAP)*, Krakow, Poland, Mar. 31–Apr. 5, 2019.
18. Wong, K. L., et al., "8-antenna and 16-antenna arrays using the quad-antenna linear array as a building block for the 3.5-GHz LTE MIMO operation in the smartphone," *Microw. Opt. Technol. Lett.*, Vol. 58, 174–181, 2016.
19. Chang, L. Y., et al., "Polarization-orthogonal co-frequency dual antenna pair suitable for 5G MIMO smartphone with metallic bezels," *IEEE Trans. Antennas Propag.*, Vol. 67, 5212–5220, 2019.
20. Abdullah, M., Y.-L. Ban, K. Kang, M.-Y. Li, and M. Amin, "Eight-element antenna array at 3.5 GHz for MIMO wireless application," *Progress In Electromagnetics Research C*, Vol. 78, 209–217, 2017.
21. Zhao, X., S. P. Yeo, and L. C. Ong, "Decoupling of inverted-F antennas with high-order modes of ground plane for 5G mobile MIMO platform," *IEEE Trans. Antennas Propag.*, Vol. 66, 4485–4495, 2018.
22. Parchin, N. O., et al., "Eight-element dual-polarized MIMO slot antenna system for 5G smartphone applications," *IEEE Access*, Vol. 9, 15612–15622, 2019.
23. Xu, S., M. Zhang, H. Wen, and J. Wang, "Deep-subwavelength decoupling for MIMO antennas in mobile handsets with singular medium," *Scientific Reports*, Vol. 7, 12162, 2017.
24. Sun, L., H. Feng, Y. Li, and Z. Zhang, "Compact 5G MIMO mobile phone antennas with tightly arranged orthogonal-mode pairs," *IEEE Trans. Antennas Propag.*, Vol. 66, 6364–6369, 2018.
25. Li, M.-Y., et al., "Tri-polarized 12-antenna MIMO array for future 5G smartphone applications," *IEEE Access*, Vol. 6, 6160–6170, 2018.
26. Zhao, A. and Z. Ren, "Size reduction of self-isolated MIMO antenna system for 5G mobile phone applications," *IEEE Antennas and Wireless Propagation Letters*, Vol. 18, 152–156, 2019.
27. Abdullah, M., et al., "High-performance multiple-input multiple-output antenna system for 5G mobile terminals," *Electronics*, Vol. 8, No. 1090, 1–16, 2019.
28. Jiang, W., B. Liu, Y. Cui, and W. Hu, "High-isolation eight-Element MIMO array for 5G smartphone applications," *IEEE Access*, Vol. 7, 34104–34112, 2019.
29. Ojaroudi, N., et al., "Enhanced bandwidth of small square monopole antenna by using inverted Ushaped slot and conductor-backed plane," *Applied Computational Electromagnetics Society (ACES) Journal*, Vol. 27, 685–690, 2012.
30. Parchin, N. O., et al., "8 × 8 MIMO antenna system with coupled-fed elements for 5G handsets," *IEEE Proceeding of Antennas and Propagation Conference*, Birmingham, UK, Nov. 2019.
31. Parchin, N. O., et al., "MM-wave phased array Quasi-Yagi antenna for the upcoming 5G cellular communications," *Applied Sciences*, Vol. 9, 1–14, 2019.
32. Abdulkhaleq, A. M., N. O. Parchin, et al., "Mutual coupling effect on three-way doherty amplifier for green compact mobile communications," *EuCAP 2020*, Copenhagen, Denmark, 2020.
33. Ojaroudi, N., et al., "An omni-directional PIFA for downlink and uplink satellite applications in C-band," *Microw. Opt. Technol. Lett.*, Vol. 56, 2684–2686, 2014.
34. Siahkhal-Mahalle, B. H., et al., "A new design of small square monopole antenna with enhanced bandwidth by using cross-shaped slot and conductor-backed plane," *Microwave Opt. Technol. Lett.*, Vol. 54, 2656–2659, 2012.
35. "Statement: Improving consumer access to mobile services at 3.6 GHz to 3.8 GHz," Available online: <https://www.ofcom.org.uk/consultations-and-statements/category-1/future-use-at-3.6-3.8-ghz>, accessed on Oct. 21, 2018.
36. *CST Microwave Studio*, ver. 2017, CST, Framingham, MA, USA, 2017.

37. Kumar, A. and S. Raghavan, "Broadband SIW cavity-backed triangular-ringslotted antenna for Ku-band applications," *AEU-International Journal of Electronics and Communications*, Vol. 87, 60-4, 2018.
38. Ojaroudi, Y., et al., "Circularly polarized microstrip slot antenna with a pair of spur-shaped slits for WLAN applications," *Microw. Opt. Technol. Lett.*, Vol. 57, 756–759, 2015.
39. Kumar, A. and S. Raghavan, "Bandwidth enhancement of substrate integrated waveguide cavity-backed bow-tie-complementary-ring-slot antenna using a shorted-via," *Defence Science Journal*, Vol. 68, 197–202, 2018.
40. Ojaroudi, N., et al., "Enhanced bandwidth of small square monopole antenna by using inverted Ushaped slot and conductor-backed plane," *Applied Computational Electromagnetics Society (ACES) Journal*, Vol. 27, No. 8, 685–690, Aug. 2012.
41. Al-Nuaimi, M. K. T. and W. G. Whittow, "Performance investigation of a dual element IFA array at 3 GHz for mimo terminals," *Antennas and Propagation Conference (LAPC)*, 1–5, Loughborough, UK, 2011.
42. Ojaroudiparchin, N., M. Shen, and G. F. Pedersen, "Small-size tapered slot antenna (TSA) design for use in 5G phased array applications," *Applied Computational Electromagnetics Society Journal*, Vol. 32, 193–202, 2018.
43. Ojaroudi, N., "Design of microstrip antenna for 2.4/5.8 GHz RFID applications," *German Microwave Conference, GeMic 2014*, RWTH Aachen University, Germany, Mar. 10–12, 2014.
44. Mazloun, J., et al., "Compact triple-band S-shaped monopole diversity antenna for MIMO applications," *Applied Computational Electromagnetics Society Journal*, Vol. 30, 975–980, 2015.
45. Ojaroudi, N. and N. Ghadimi, "Design of CPW-fed slot antenna for MIMO system applications," *Microw. Opt. Technol. Lett.*, Vol. 56, 1278–1281, 2014.
46. Valizade, A., et al., "Band-notch slot antenna with enhanced bandwidth by using Ω -shaped strips protruded inside rectangular slots for UWB applications," *Appl. Comput. Electromagn. Soc. (ACES) J.*, Vol. 27, 816–822, 2012.
47. Ojaroudi, N., et al., "Compact ultra-wideband monopole antenna with enhanced bandwidth and dual band-stop properties," *International Journal of RF and Microwave Computer-Aided Engineering*, 346–357, 2014.
48. Khan, R., A. A. Al-Hadi, and P. J. Soh, "Recent advancements in user effect mitigation for mobile terminal antennas: A review," *IEEE Trans. Electromagn. Compat.*, Vol. 61, No. 1, 279–287, Feb. 2019.
49. Khan, R., et al., "User influence on mobile terminal antennas: A review of challenges and potential solution for 5G antennas," *IEEE Access*, Vol. 6, 77695–77715, 2018.
50. Sharawi, M. S., "Printed multi-band MIMO antenna systems and their performance metrics [wireless corner]," *IEEE Antennas Propag. Mag.*, Vol. 55, 218–232, 2013.
51. Ojaroudiparchin, N., M. Shen, and G. F. Pedersen, "Design of Vivaldi antenna array with end-fire beam steering function for 5G mobile terminals," *23rd Telecommunications Forum Telfor (TELFOR)*, 587–590, Belgrade, Serbia, Nov. 24–26, 2015.
52. Parchin, N. O., et al., "Multi-band MIMO antenna design with user-impact investigation for 4G and 5G mobile terminals," *Sensors*, Vol. 19, 456, 2019.
53. Srytsin, I., S. Zhang, and G. F. Pedersen, "Performance investigation of a mobile terminal phased array with user effects at 3.5 GHz for LTE advanced," *IEEE Antennas and Wireless Propagation Letters*, Vol. 16, 1847–1850, 2017.
54. Ojaroudiparchin, N., et al., "A switchable 3-D-coverage-phased array antenna package for 5G mobile terminals," *IEEE Antennas Wireless Propag. Lett.*, Vol. 15, 1747–1750, 2016.
55. Isa, C. M. N. C., A. A. Al-Hadi, S. N. Azemi, A. M. Ezanuddin, H. Lago, and M. F. Jamlos, "Effects of hand on the performance of 5 GHz two port terminal antennas," *Proc. IEEE Asia-Pacific Conf. Appl. Electromagn. (APACE)*, 207–210, Dec. 2016.